Comparative Study of Reservoir Simulation Tools with Application of Hydrogen Underground Storage at the Ketzin Site

Anna-Maria Eckel[*,1], Lea Döpp[1,2], Márton Pál Farkas[1], Cornelia Schmidt-Hattenberger[1], and Ingo Sass[1,2]

[1] GFZ Helmholtz Centre Potsdam, German Research Centre for Geosciences, Section 4.8 Geoenergy, Telegrafenberg, 14473 Potsdam, Germany
[2] Technical University Darmstadt, Institute of Applied Geosciences, Geothermal Science and Technology, Schnittspahnstraße 9, 64287 Darmstadt, Germany
[*]Corresponding author: eckel@gfz-potsdam.de

Abstract. With the growing interest in hydrogen as a clean energy carrier, understanding underground hydrogen storage subsurface behaviour is crucial for successful implementation. Thereby, reservoir simulations offer critical insights into reservoir characteristics like storage capacity, pressure dynamics, and gas migration routes, making them indispensable for evaluating, enhancing, and monitoring gas storage systems. This study presents a comparative analysis of two distinct reservoir simulation tools, evaluating their results in simulating the injection and storage of hydrogen at the former gas storage site of Ketzin in Germany. Compared are the results of a commercial simulator (CMG GEM) and an open-source option (MUFITS). Results show good agreement between the model results in various parameters such as plume spreading and bottom hole pressure. This study demonstrates the confidence in using an open-source simulator as an alternative to commercial solutions.

Keywords: underground hydrogen cyclic storage, saline aquifer, gas storage, numerical reservoir simulation tools

1 Introduction

As renewable energies, like solar and wind, gain importance, hydrogen (H_2) emerges as a vital energy carrier for transitioning to a cleaner economy, storing excess energy via electrolysis and addressing fluctuations in electricity transmission. Forecasts indicate a substantial surge in hydrogen demand by 2050, potentially reducing greenhouse gas emissions in the EU energy system by at least 90 % [1]. For the realisation of these targets, cost-effective energy storage solutions are crucial. Geological options for underground hydrogen storage (UHS), such as saline aquifers and salt caverns, are effective for large-scale, seasonal needs and offer ample capacity and enhanced safety compared to aboveground facilities [2]. For instance, in saline aquifers, the hydrogen will be stored in the pore spaces of the reservoir, enabling its extraction and utilisation during

periods of high power demand. Given the complexity of such gas storage systems, numerical reservoir simulations are essential for optimising gas injection and production strategies, ensuring reservoir integrity, and maximizing storage capacity. Reservoir simulations predict pressure and temperature distributions, model various scenarios, and aid in understanding fluid flow dynamics [3, 4].

History matching, a common method to set up subsurface flow models for instance in natural gas storage [5, 6, 7], is not a feasible concept for H_2 storage modeling because of the lack of historical data, specific to pure H_2 storage. Other ways for cross-validation to gain confidence in the results obtained from simulation tools are required. In various contexts such as carbon dioxide (CO_2) storage [8, 9] or enhanced oil recovery [10, 11], comparing the results of different simulators are a frequently used method. In this study, the comparison is focused on finite-difference-based simulators: the open-source simulator MUFITS [12] and the commercial software CMG GEM [13] are applied. Open-source simulators provide cost-effective solutions with their accessibility, collaborative development and adaptable nature compared to commercial solutions. This study aims to assess whether this versatile open-source tool can reliably replicate the outcomes achieved by a commercial simulator. We aim to discern any discrepancies or similarities in the outcomes, thereby evaluating the reliability of the results obtained. We apply a geological model of the Upper Triassic Stuttgart Formation of the Ketzin site in North-East Germany and simulate a cyclic hydrogen injection and production process of roughly 5 years. The Ketzin saline aquifer site is a historic gas storage site and the location of Europe's first onshore CO_2 storage project [14, 15, 16]. The decades of experience in gas operations and the established infrastructure at the Ketzin site underline the potential for H_2 storage tests. The ongoing research project *GEOZeit* of the Helmholtz Association of German Research Centres is dedicated to the preliminary investigations required to evaluate the suitability of the Ketzin saline aquifers for the construction of an underground hydrogen demonstrator.

In this study, we first present an overview of the applied simulators MUFITS and CMG GEM, alongside the geological model and the input data utilized (Section 2). For the comparison of the results various parameters are used, encompassing the bottom hole pressure (BHP), injection and production rates and total masses as well as the production of brine. Further, the gas plume shape and spreading are assessed by comparing the gas saturation distribution over time (Section 3). This is followed by a combined discussion and conclusion (Section 4).

2 Methodology

2.1 Applied Numerical Simulators

The simulations are conducted using the open-source simulator MUFITS and commercial software CMG GEM. MUFITS is a noncommercial reservoir simulator and aims to analyse non-isothermal multiphase multicomponent flows in porous media [8, 12]. MUFITS was chosen because it has previously demonstrated successful performance in geological reservoir modelling for CO_2 storage

within the Ketzin saline aquifer [17, 18]. CMG GEM is a widely-used commercial software for gas storage simulations, extensively employed in both industry and research (*e.g.*, [19, 20, 21, 22]). It was shown that CMG GEM is proficient in handling hydrogen gas within the PVT model and a precise simulation of multiphase flow, hysteresis, and fluid behaviour was demonstrated [23].

In Table 2.1 the essential numerical details of the two simulators are listed. Both work with equation of state (EOS) modules and use finite-difference and finite-volume schemes as numerical techniques. Identical geological structures, input parameters, and boundary conditions outlined in Section 2.2, 2.3 and 2.4 are applied. However, while both tools utilize a Peng Robinson equation as EOS, MUFITS incorporates the Søreide and Whitson modification [24] of the Peng Robinson equation. Furthermore, although the time-stepping schemes share similarities, they are not entirely identical.

Table 2.1. Essential details of the methods and models applied in the numerical simulators. The reader can refer to the respective manuals for further information [12, 13].

	MUFITS model	**CMG GEM model**
Numerical method	finite-difference and -volume	finite-difference and -volume
Applied Module	COMPS	GEM
Flow equation	Darcy's law	Darcy's law
EOS	Søreide Whitson (modified Peng Robinson)	Peng Robinson
Dissolution (H_2 in brine)	included in EOS	solubility model
Run time	approx. 30 min (workstation, 8 cores)	approx. 1 min (workstation, 16 cores)
Solver	linear solver	linear solver

2.2 Geological Model

We employed a static geological model from the CO_2SINK Petrel model [25], measuring about 3000 m × 2500 m with a total thickness of approximately 85 m. The simulation covers a storage formation thickness of around 70 m (533 m to 664 m depth, see Figure 2.1b) beneath a 15 m thick caprock. The model grid from Norden and Frykman (2013) [25] was adapted while a coarsening procedure of the reservoir and a refining procedure near the injection point was conducted. The in this study applied grid is shown in Figure 2.1a. Five vertical faults intersect the Stuttgart Formation [14] which are depicted also in Figure 2.1a. A single well, used for injection and production, is positioned at the top of the anticline (2 km north of the former CO_2 injection site, for positioning refer to Figure 2.1a and b) and is perforated from below the caprock till the deepest point of the reservoir.

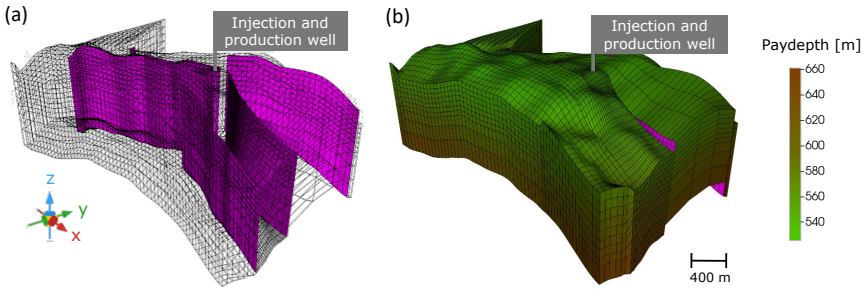

Fig. 2.1. The spatial discretisation of the Ketzin anticline used for the numerical simulations. The figures are extracted from CMG GEM. The grid consists of 22 040 elements. The z-direction is magnified 10 times. (a) Shown is the grid structure with a visualisation of the fault structures in purple colour. (b) Depicted is the paydepth as reservoir property.

We assume for this study that the reservoir is uniform and homogeneous while the permeability is showing an anisotropy. The geological parameters applied in the reservoir are shown in Table 2.2. Because of limited data availability regarding relative permeability and capillary pressure for H_2 gas, we incorporate the experimental findings from Fleury et al. (2013) [26], which are derived from experiments conducted with CO_2 using Ketzin rock samples. Hysteresis in relative permeability and capillary pressure are not considered.

Table 2.2. Geological and reservoir parameters applied in the numerical simulations.

Parameter	**Value**
Reservoir porosity [−]	0.2
Reservoir horizontal permeability [mD]	260.0
Reservoir vertical permeability [mD]	86.6
Salinity [mol/kg]	3.5
Isothermal condition [°C]	33

2.3 Numerical Setup

The reservoir is modelled as laterally open and effectively sealed at the bottom by imposing no-flow and no-flux boundary conditions. For this study, the caprock and the faults are assumed to be impermeable and closed to flow and transport. For the isothermal simulation, an average temperature of 33 °C is assumed uniformly throughout the formation. Initially, all cells are fully saturated

with water, no gas is present in the reservoir and the average pore pressure applied is 55 bar. During operational phases (B-D), solution time steps range from 2 days to 300 days.

2.4 UHS Operation Cycles

In this study, H_2 is the working gas, while nitrogen (N_2) is the cushion gas. Injection and production pressures are capped at 85 bar and 48 bar, respectively. The total simulated time is 5.1 years and the operative phases follow the ones of Pfeiffer and Bauer (2015) [27] and are shown as color-coded blocks in Figure 2.2. For more details please refer to the caption of the figure.

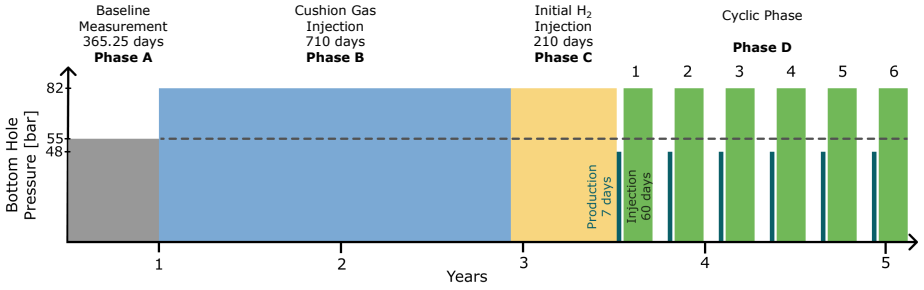

Fig. 2.2. Schematic representation of the operative phases and the respective input BHP pressures at the well. No BHP pressure is set during the well stop periods between the injection and production cycles.
(A) Baseline period representing the time period needed for baseline measurements during the construction of a demonstrator storage site (assumed 1 year).
(B) Period of N_2 cushion gas injection (710 days).
(C) Initial H_2 injection period (210 days).
(D) Cyclic phase consisting of a production period (7 days) and a H_2 injection period (60 days) [27].

3 Results

In this section, we will contrast the outcomes generated by the two simulators, utilizing a variety of result parameters for comparison. The success of the matching is discussed based on the proximity of the results obtained from each simulator.

3.1 Bottom Hole Pressure

In comparing bottom hole pressure (BHP) results between MUFITS and CMG GEM in Figure 3.3, it is evident that due to the BHP being an input parameter, identical results occur when pressure remains constant. However, during intervals between injection and production, the BHP still demonstrates remarkable agreement. The difference between the two simulator results is minimal, below 1.0%, indicating a high level of consistency during well-stop periods (all percentages are based on MUFITS values). During the baseline measurement period (A), no BHP is set, and the pressure depicted in the diagram represents the pore pressure within the reservoir. The slight variance between the two simulator results arises from the slightly different positions in the well used for measuring reservoir pressure.

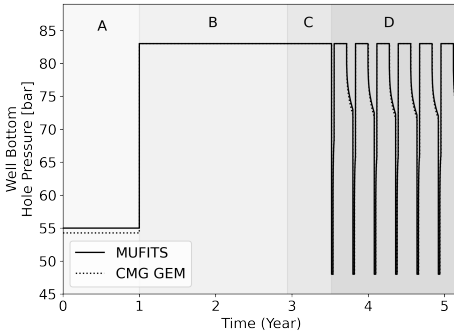

Fig. 3.3. Output BHP pressures from the MUFITS (solid lines) and the CMG GEM simulator (dashed lines). A period of constant BHP represents a time when the pressure is set in the model and injection or production is operated. The different operational phases are marked with capital letters A-D according to Figure 2.2 and colour-coded with increasing shades of grey.

3.2 Development of Gas Saturation and Spreading of Gas Plume

A vertical cut in along the x-z plane and through the injection point is shown in Figure 3.4 for both models after the last production cycle. The gas distribution is shown as gas saturation S_g. The remarkably high similarity is evident when comparing the plume distribution, plume size and the respective gas saturation visually. In both cases, the plume shows a cone-like shape due to buoyancy effects, with the widest spread at the top and the smallest at the bottom of the reservoir. The highest values are close to the well and close to the sealed caprock ($S_\mathrm{g} = 0.5$-0.6).

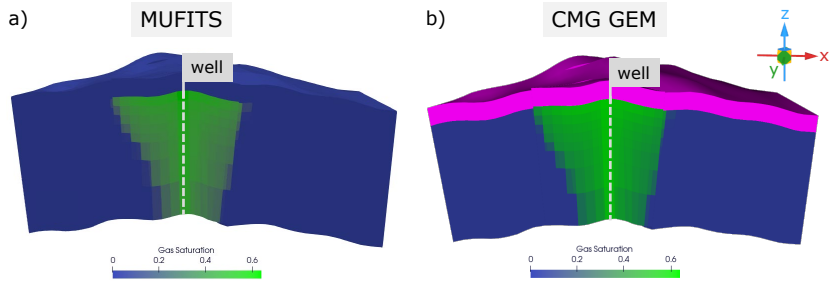

Fig. 3.4. Cross section of a plume of (a) MUFITS and (b) CMG GEM. The vertical cut is located a the position of the well in the x-z plane. The gas distribution is shown in terms of gas saturation S_g at the last time step. No gas enters the caprock as it is modelled as a non-permeable layer in MUFITS (caprock coloured as $S_g = 0$). In CMG GEM the caprock is defined as inactive cells, non-permeable cells, which are colored in pink by the software.

To further evaluate the lateral spread of the gas plume, we examine snapshots of an aerial view as depicted in Figure 3.5. Across the four instances examined, we observe a consistent pattern. In both cases, the gas plume expands with time but encounters a barrier in y-direction due to the impermeable faults. At the location where the fault is discontinuous, the plume is allowed for further expansion in y-direction. The gas saturation is high near the location of the well but even near the periphery of the gas plume, it persists around $S_g \approx 0.5$. We observe very strong similarities by visual comparison between the Figures 3.5 on the left panel (MUFITS) and the right panel (CMG GEM) in terms of local plume propagation as well as gas saturation.

3.3 Gas Injection and Production

Figure 3.6 depicts nitrogen injection rates (a) and cumulative injection trends over time (b) derived from both MUFITS and CMG GEM models. Upon comparing the total injected N_2 masses, CMG yielded a 0.1 % lower value compared to MUFITS (50142 t of N_2). The relative error in the time-weighted average of N_2 injection rates diverged also by 0.1 % between the MUFITS and CMG simulations. The comparison indicates that the results obtained in the first injection period (cushion gas injection) simulations show very high agreement in both, the injection rate and total injected mass.

This is followed by the initial H_2 injection and continues by the cyclic injection and production of H_2. We observe a higher contrast between the two model results in the total injected mass of H_2 compared to N_2. For instance, after the first cycle (Figure 3.7a, after 3.7 years), the total injected mass of H_2 amounts to 2277 t in CMG and 1734 t in MUFITS, representing a difference of 31.3 %. This difference slightly decreased to 22.9 % after the last cycle. Considering the amount of produced H_2 gas (Figure 3.7b), CMG yields a value of 994 t of H_2

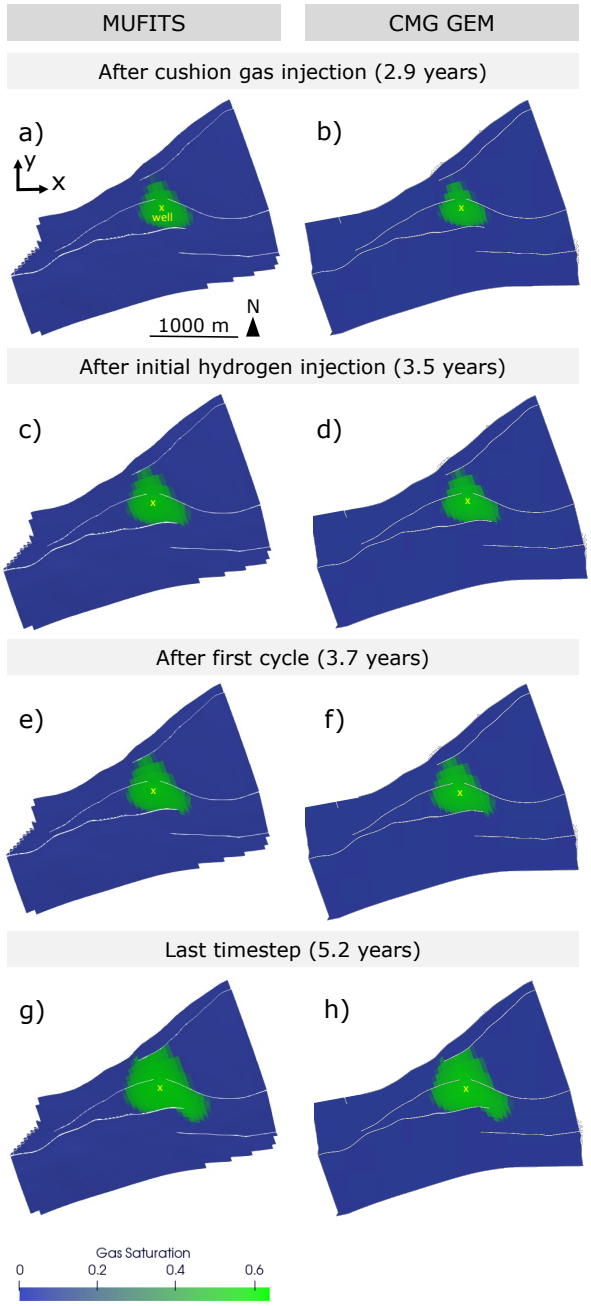

Fig. 3.5. Development of gas plume over four distinct times of the simulation. Shown is the aerial view of the layer right below the caprock for the MUFITS and the CMG GEM results.

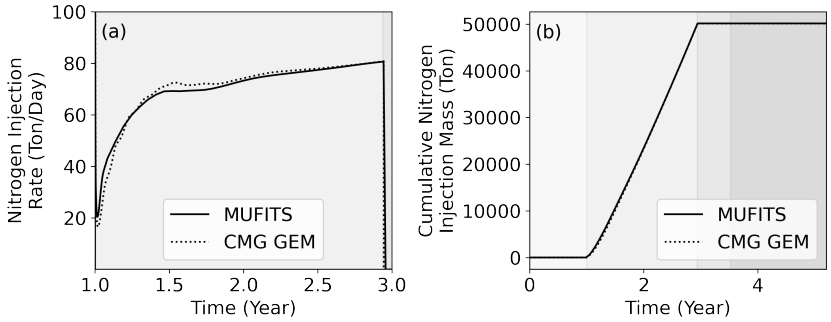

Fig. 3.6. (a) Nitrogen injection rates in the two years of cushion gas injection and (b) cumulative nitrogen injection mass over total time. Solid lines represent the MUFITS results and the dashed lines the CMG results.

after the total simulated time while MUFITS provides again a lower result of 898 t which makes up a difference of 10.7 %.

In Figure 3.7c, the results of the gas rates of the first operation cycle after the initial H_2 injection period are depicted. We opted to display the first cycle since rates are less affected by discrepancies from the proceedings phases. In terms of the operative phases of the first cycle (Figure 3.7c), the H_2 injection and production rates of CMG are higher than the ones of MUFITS by roughly 20 % and 13 %, respectively (compared are the values of the last time step of the respective phases). However, we observe the opposite in the N_2 production rate and the MUFITS model gives a production rate that is roughly double the one of the CMG model. Since N_2 is injected first as the cushion gas, it encompasses the H_2 gas plume. Therefore, H_2 is the dominant gas close to the well, making the N_2 production values more sensitive to discrepancies between the models. In other words, while both models enable a highly comparable level of N_2 injection, the CMG model permits greater H_2 injection and production, both per cycle and cumulatively. Therefore, we anticipate a reduced fraction of H_2 in the gas stream produced by MUFITS compared to CMG GEM due to lower gas production masses of H_2, leading to a slightly diminished cyclic gas storage performance of the MUFITS simulator.

3.4 Total Mass of Brine Production

Figure 3.8 displays the cumulative brine production over time of both, the MUFITS model and the CMG GEM model. By comparing these cumulative profiles, more insights into the efficiency and performance of the UHS operation can be gained and compared between the two simulators. Although we demonstrate very similar gas saturation in vertical and horizontal directions of the gas plume (Figures 3.4 and 3.5), even slight disparities near the perforated well gradually

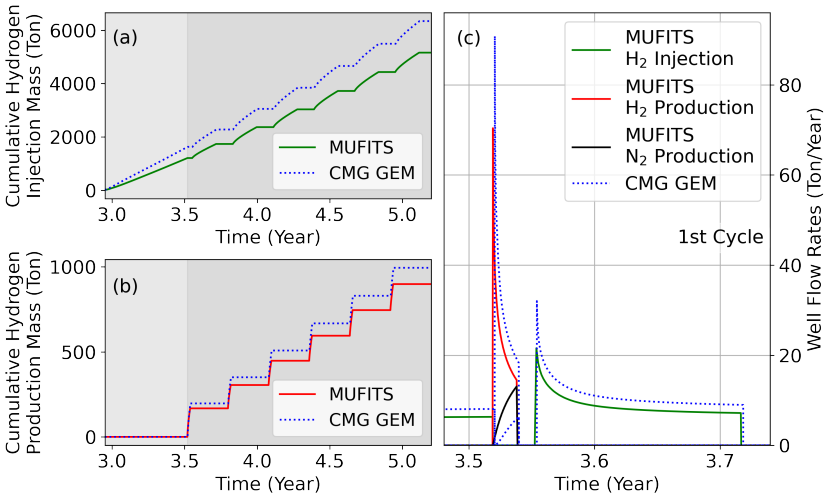

Fig. 3.7. (a) Cumulative hydrogen injection mass over time, (b) cumulative hydrogen production mass over time, (c) well flow rates over time of the first cycle. Solid lines represent the MUFITS results and the dashed lines the respective CMG results of that operative period. The first cycle starts after the initial H_2 injection at a time of 3.5 years.

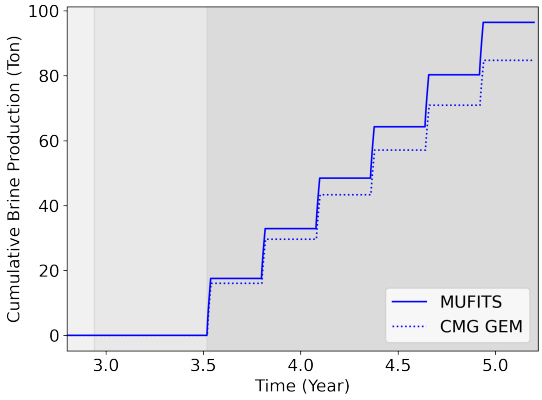

Fig. 3.8. Cumulative brine production over time of the two simulators MUFITS and CMG GEM.

accumulate over time, leading to moderate variations in the mass of produced water of 8.6 % in the first cycle and 14.3 % in the last cycle.

4 Discussion and Conclusion

In this study, we compare the results of the open-source reservoir simulator MUFITS with results from an equivalent model using the commercial CMG GEM compositional simulator. Identical input data and geological models are applied in both models. The analysis reveals a high level of concordance between the simulators, particularly evident in the matching of plume spreading, bottom hole pressure (BHP) and mass of injected cushion gas (N_2). The total mass of injected and produced H_2, along with the total mass of brine, exhibits good agreement. However, there is a discrepancy in the matching regarding N_2 production, with the CMG model indicating lower N_2 production values. We expect that the modifications in the EOS contribute to this discrepancy between the model results. While in CMG the Peng-Robinson equation of state is applied, in the MUFITS model the Søreide and Whitson EOS is used. The Søreide and Whitson EOS is developed from the Peng Robinson equation but includes modifications to adjust for salinity effects [28]. While the time-stepping scheme of the two model solutions is not identical, we anticipate minimal impact on the results since the chosen time steps are sufficiently small to mitigate any significant influence on the outcomes.

Overall, the comparison demonstrates a strong agreement of the total injected N_2 ("gas in liquid injection") of less than 1 % difference between the model results. However, as the operation progresses into the cyclic H_2 injection phase ("gas in gas injection"), the variance intensifies. Nevertheless, the overall variance in the total H_2 production remains within 11 % between the model predictions. Therefore, we conclude that the comparison using an H_2 storage process in a realistic geological environment demonstrated a robust similarity between the results generated by the models and that the open-source simulator MUFITS delivers reliable results, establishing itself as a viable option among non-commercial simulator solutions.

Acknowledgments

The authors thank Prof. Dr. Hannes Hofmann from GFZ Helmholtz Centre Potsdam for the valuable discussions and support with the software.

This research work was funded within the Helmholtz project GEOZeit by the Federal Ministry of Education and Research, Germany.

Statement

During the preparation of this work, the authors used the tools *Grammarly, Inc.* and *ChatGPT* for language validation and refinement. After using those tools, the authors reviewed and edited the content as needed and take full responsibility for the content of the publication.

Bibliography

[1] M. Wietschel, L. Zheng, M. Arens, C. Hebling, O. Ranzmeyer, A. Schaadt, C. Hank, A. Sternberg, S. Herkel, C. Kost, M. Ragwitz, U. Herrmann, B. Pfluger, Metastudie Wasserstoff – Auswertung von Energiesystemstudien. Studie im Auftrag des Nationalen Wasserstoffrats, 2021.

[2] D. Zivar, S. Kumar, J. Foroozesh, Underground hydrogen storage: A comprehensive review, International Journal of Hydrogen Energy 46 (2021) 23436–23462. doi:10.1016/j.ijhydene.2020.08.138.

[3] B. Sørensen, Geological hydrogen storage, World Hydrogen Technologies Convention 2007 (2007). URL: https://rucforsk.ruc.dk/ws/portalfiles/portal/3503367/Geological_hydrogen_storage.pdf.

[4] M. Delshad, Y. Umurzakov, K. Sepehrnoori, P. Eichhubl, B. R. Batista Fernandes, Hydrogen storage assessment in depleted oil reservoir and saline aquifer, Energies 15 (2022) 8132. doi:10.3390/en15218132.

[5] E. Khamehchi, F. Rashidi, Simulation of underground natural gas storage in Sarajeh gas field, Iran, in: All Days, SPE, 05212006. doi:10.2118/106341-MS.

[6] J. Ory, K. Guedeney, B. Brefort, L. Schirrer, A semi-automatic history matching technique applied to aquifer gas storages, SPE Annual Technical Conference and Exhibition (1997). doi:10.2118/38862-MS.

[7] T. Aurdal, N. Cheng, J. Muller, J. Sagen, History matching of gas tracer data to identify and estimate gas storage volumes in a north sea oil field, 2001.

[8] A. Afanasyev, T. Kempka, M. Kühn, O. Melnik, Validation of the MUFITS reservoir simulator against standard industrial simulation tools for CO_2 storage at the Ketzin pilot site: Geophysical research abstracts, EGU General Assembly 2016 (2016).

[9] B. Flemisch, J. M. Nordbotten, M. Fernø, R. Juanes, J. W. Both, H. Class, M. Delshad, F. Doster, J. Ennis-King, J. Franc, S. Geiger, D. Gläser, C. Green, J. Gunning, H. Hajibeygi, S. J. Jackson, M. Jammoul, S. Karra, J. Li, S. K. Matthäi, T. Miller, Q. Shao, C. Spurin, P. Stauffer, H. Tchelepi, X. Tian, H. Viswanathan, D. Voskov, Y. Wang, M. Wapperom, M. F. Wheeler, A. Wilkins, A. A. Youssef, Z. Zhang, The fluidflower validation benchmark study for the storage of CO_2, Transport in Porous Media 151 (2024) 865–912. doi:10.1007/s11242-023-01977-7.

[10] A. Goudarzi, M. Delshad, K. Sepehrnoori, A critical assessment of several reservoir simulators for modeling chemical enhanced oil recovery processes, SPE Reservoir Simulation Symposium (2013). doi:10.2118/163578-MS.

[11] A. Goudarzi, M. Delshad, K. Sepehrnoori, A chemical EOR benchmark study of different reservoir simulators, Computers & Geosciences 94 (2016) 96–109.

[12] A. Afanasyev, MUFITS. Release 2022.B. Reference Manual (2023).

[13] User's guide GEM: Advanced compositional and ghg reservoir simulator: Version 2023, 2023.

[14] C. Juhlin, R. Giese, K. Zinck-Jørgensen, C. Cosma, H. Kazemeini, N. Juhojuntti, S. Lüth, B. Norden, A. Förster, 3D baseline seismics at Ketzin, Germany: The CO_2SINK project, GEOPHYSICS 72 (2007) B121–B132. URL: https://library.seg.org/doi/10.1190/1.2754667. doi:10.1190/1.2754667.

[15] C. Lubitz, T. Kempka, M. Motagh, Integrated assessment of ground surface displacements at the Ketzin pilot site for CO_2 storage by satellite-based measurements and hydromechanical simulations, IEEE Journal of Selected Topics in Applied Earth Observations and Remote Sensing 12 (2019) 186–199. doi:10.1109/JSTARS.2018.2886637.

[16] GFZ, Pilotstandort Ketzin: Startseite, 09.02.2024. URL: https://www.co2ketzin.de/startseite.

[17] E. Kanin, I. Garagash, S. Boronin, S. Zhigulskiy, A. Penigin, A. Afanasyev, D. Garagash, A. Osiptsov, CO_2 storage in deep saline aquifers: evaluation of geomechanical risks using integrated modeling workflow, arXiv, 2023. URL: https://www.researchgate.net/profile/evgenii-kanin/publication/367088563_co2_storage_in_deep_saline_aquifers_evaluation_of_geomechanical_risks_using_integrated_modeling_workflow. doi:10.48550/arXiv.2301.04931.

[18] A. A. Afanasyev, Application of the reservoir simulator MUFITS for 3D modelling of CO_2 storage in geological formations, 1876-6102 40 (2013) 365–374. URL: https://www.sciencedirect.com/science/article/pii/s1876610213016366. doi:10.1016/j.egypro.2013.08.042.

[19] P. Jadhawar, M. Saeed, Mechanistic evaluation of the reservoir engineering performance for the underground hydrogen storage in a deep North Sea aquifer, 0360-3199 50 (2024) 558–574. URL: https://www.sciencedirect.com/science/article/pii/s0360319923038235. doi:10.1016/j.ijhydene.2023.07.272.

[20] S. V. Solano, J.-P. Nicot, S. A. Hosseini, Sensitivity study of CO_2 storage in saline aquifers in the presence of a gas cap, 1876-6102 4 (2011) 4508–4515. URL: https://www.sciencedirect.com/science/article/pii/s1876610211006862. doi:10.1016/j.egypro.2011.02.407.

[21] R. Ershadnia, M. Singh, S. Mahmoodpour, A. Meyal, F. Moeini, S. A. Hosseini, D. M. Sturmer, M. Rasoulzadeh, Z. Dai, M. R. Soltanian, Impact of geological and operational conditions on underground hydrogen storage, International Journal of Hydrogen Energy 48 (2023) 1450–1471. doi:10.1016/j.ijhydene.2022.09.208.

[22] Ö. İ. Özkılıç, F. Gumrah, Simulating CO_2 sequestration in a depleted gas reservoir, Energy Sources, Part A: Recovery, Utilization, and Environmental Effects 31 (2009) 1174–1185. doi:10.1080/15567030801952235.

[23] M. Bahrami, E. Izadi Amiri, D. Zivar, S. Ayatollahi, H. Mahani, Challenges in the simulation of underground hydrogen storage: A review of relative permeability and hysteresis in hydrogen-water system, Journal of Energy Storage 73 (2023) 108886. doi:10.1016/j.est.2023.108886.

[24] I. Søreide, C. H. Whitson, Peng-robinson predictions for hydrocarbons, CO_2, N_2 and H_2S, with pure water and NaCl brine, Fluid Phase Equilibria 77 (1992) 217–240. URL: https://www.sciencedirect.com/science/article/pii/037838129285105h. doi:10.1016/0378-3812(92)85105-H.

[25] B. Norden, P. Frykman, Geological modelling of the Triassic Stuttgart formation at the Ketzin CO_2 storage site, Germany, International Journal of Greenhouse Gas Control 19 (2013) 756–774. URL: https://www.sciencedirect.com/science/article/pii/S1750583613001989. doi:10.1016/j.ijggc.2013.04.019.

[26] M. Fleury, S. Gautier, N. Gland, P. F. Boulin, B. Norden, C. Schmidt-Hattenberger, Advanced and integrated petrophysical characterization for CO_2 storage: Application to the Ketzin site, Oil & Gas Science and Technology – Revue d'IFP Energies nouvelles 68 (2013) 557–576. URL: http://ogst.ifpenergiesnouvelles.fr/10.2516/ogst/2012084. doi:10.2516/ogst/2012084.

[27] W. T. Pfeiffer, S. Bauer, Subsurface porous media hydrogen storage – scenario development and simulation, 1876-6102 76 (2015) 565–572. URL: https://linkinghub.elsevier.com/retrieve/pii/S1876610215016483. doi:10.1016/j.egypro.2015.07.872.

[28] A. Afanasyev, E. Vedeneeva, Compositional modeling of multicomponent gas injection into saline aquifers with the mufits simulator, Journal of Natural Gas Science and Engineering 94 (2021) 103988. URL: https://linkinghub.elsevier.com/retrieve/pii/S1875510021001955. doi:10.1016/j.jngse.2021.103988.